Supplementary information for

Facile discovery of a therapeutic agent for NK-mediated synergistic antitumor effects using a patient-derived 3D Platform

Young Eun Lee,[‡a,b] Chae Min Yuk,[‡a] Minseok Lee,[‡c] Ki-Cheol Han,[a] Eunsung Jun,[d,e] Tae Sung Kim,[b] Ja-Lok Ku,[f] Sung G. Im,*[c] Eunjung Lee*[c] and Mihue Jang*[a,g]

[a]Theragnosis Research Center, Biomedical Research Division, Korea Institute of Science and Technology, Seongbuk-Gu, Seoul 02792, Republic of Korea

[b]Department of Life Sciences, College of Life Sciences and Biotechnology, Korea University, Seoul 02841, Republic of Korea

[c]Department of Chemical and Biomolecular Engineering, Korea Advanced Institute of Science and Technology, Daejeon 34141, Republic of Korea

[d]Department of Convergence Medicine, Asan Institute for Life Sciences, University of Ulsan College of Medicine and Asan Medical Center, Seoul 05505, Republic of Korea

[e]Division of Hepato-Biliary and Pancreatic Surgery, Department of Surgery, University of Ulsan College of Medicine, Asan Medical Center, Seoul 05505, Republic of Korea

[f]Korean Cell Line Bank, Laboratory of Cell Biology, Cancer Research Institute, Seoul National University College of Medicine, Seoul 03080, Republic of Korea

[g]KHU-KIST Department of Converging Science and Technology, Kyung Hee University, Seoul 02447, Republic of Korea

[‡]These authors contributed equally to this work

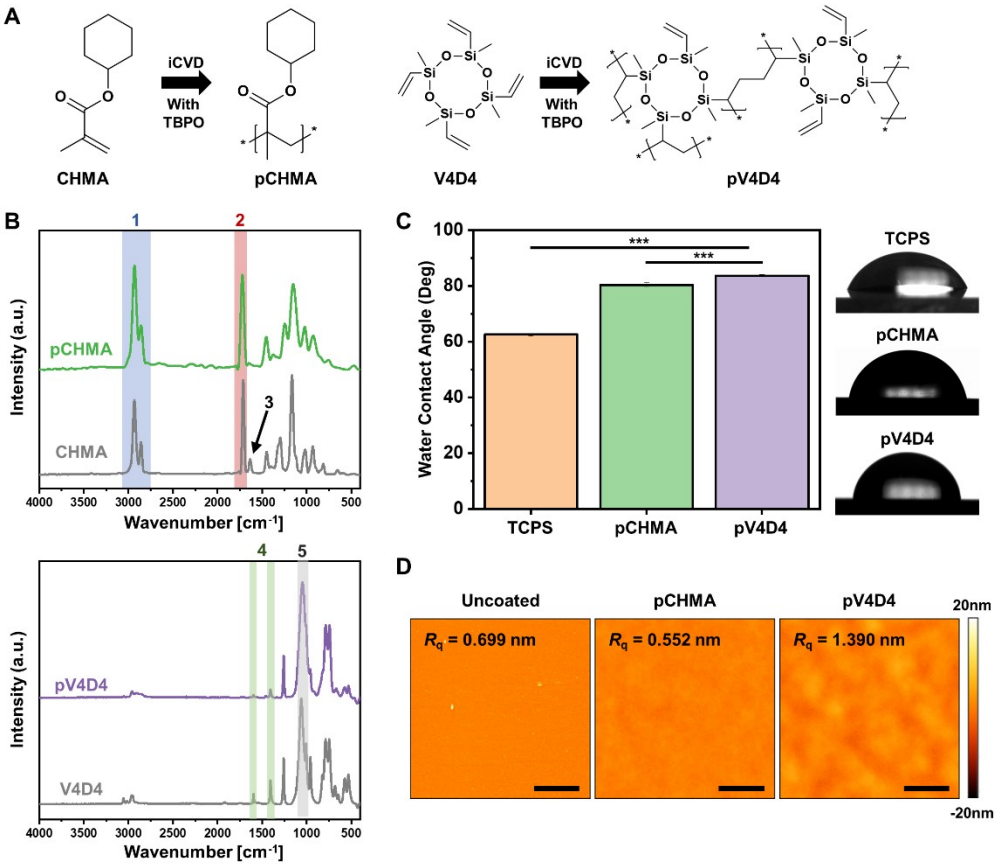

Figure S1. Characterization of polymer films synthesized through iCVD process. (A) Illustration of the synthetic scheme of pCHMA and pV4D4. (B) The FT-IR spectra of the polymers (1: -CH_2- symmetrical and asymmetrical cyclohexyl vibration peak, 2: -C=O stretching peak, 3: C=C vinyl peak, 4: C=C stretching peaks, 5: Si-O-Si peaks) (C) Water contact angle values (n = 3) and images. (D) AFM images and the measured RMS roughness (R_q) (Scale bar = 1 μm).

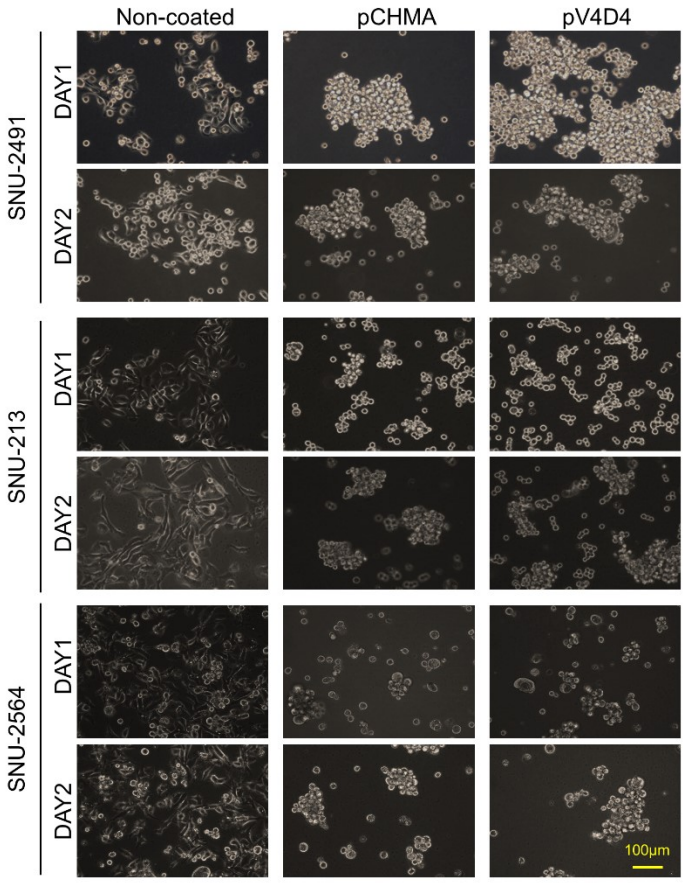

Figure S2. Cell aggregate morphologies of non-spheroid forming PDCs, using two types of hydrophobic polymers, pCHMA and pV4D4, were shown by optical microscopy. Scale bar indicates 100 μm.

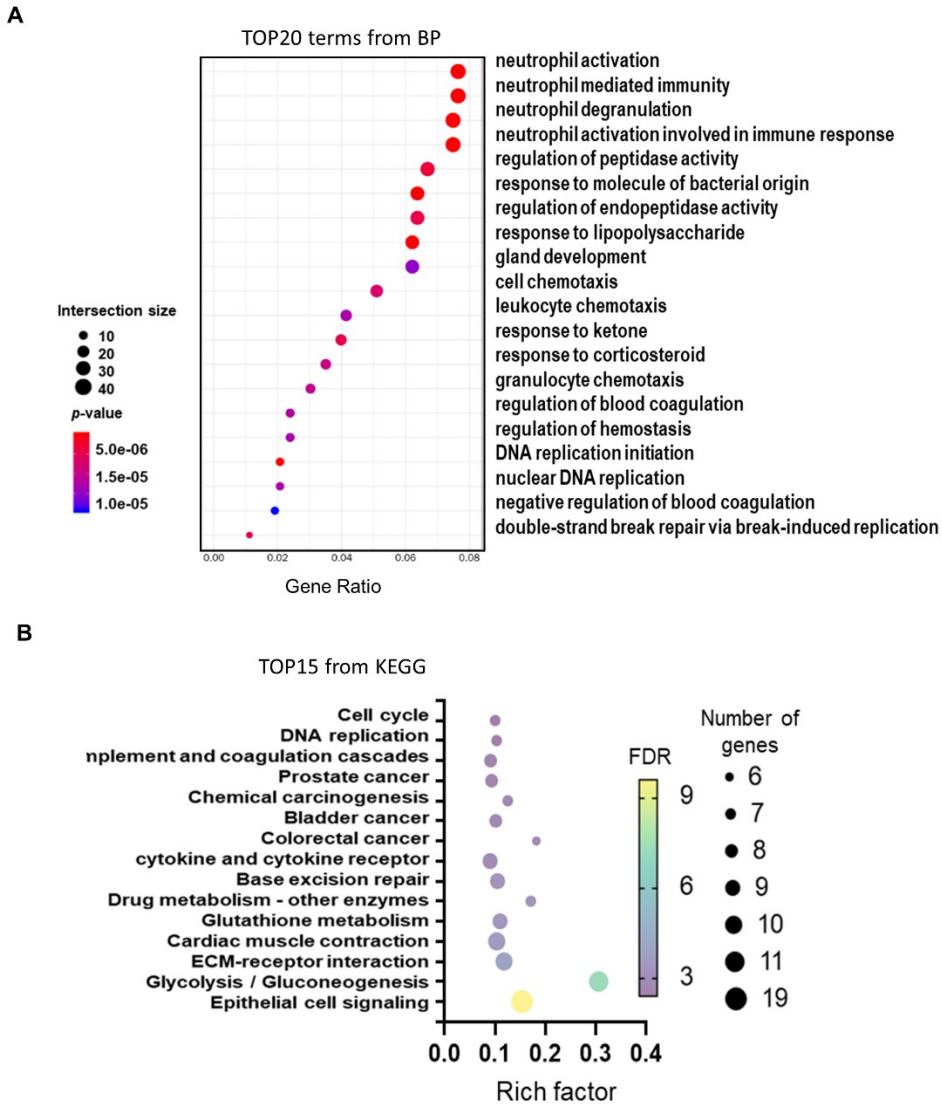

Figure S3. GO biological process pathway (A) and KEGG enrichment pathway analyses (B) based on WTS. DEGs were analyzed in 3D spheroids of 110621 and SNU2608 compared to the 2D cell culture conditions

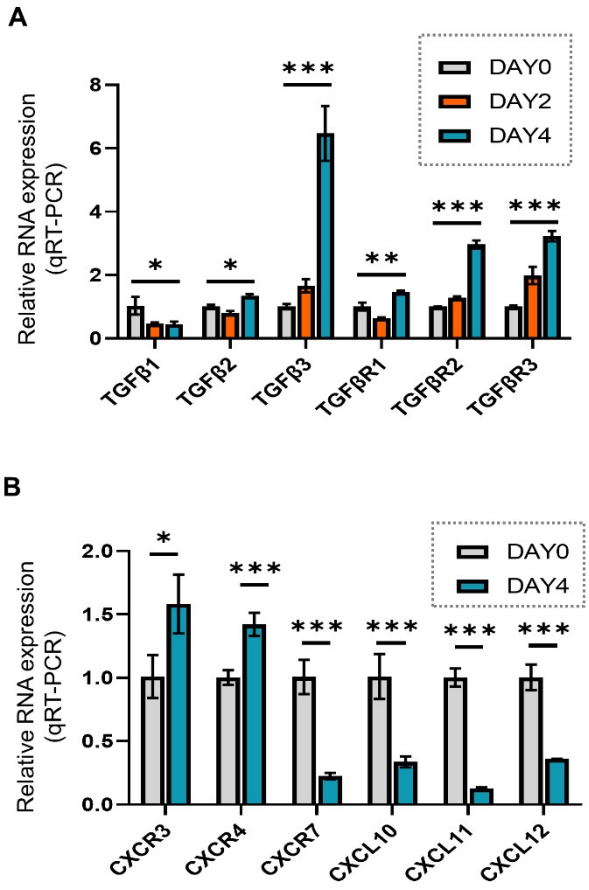

Figure S4. Expression levels of genes involved in ECM modeling and EMT function as measured by qRT- PCR in a 3D PDC spheroids. (A) The expression of TGF-β cytokines and their receptors are shown. (B) The expression of chemokines and chemokine receptors are depicted. The p values were determined using a one-way ANOVA test followed by Tukey's multiple comparison test (A) or an unpaired Student's *t*-test (B). **p* <0.05; ***p* <0.01; ****p* <0.001.

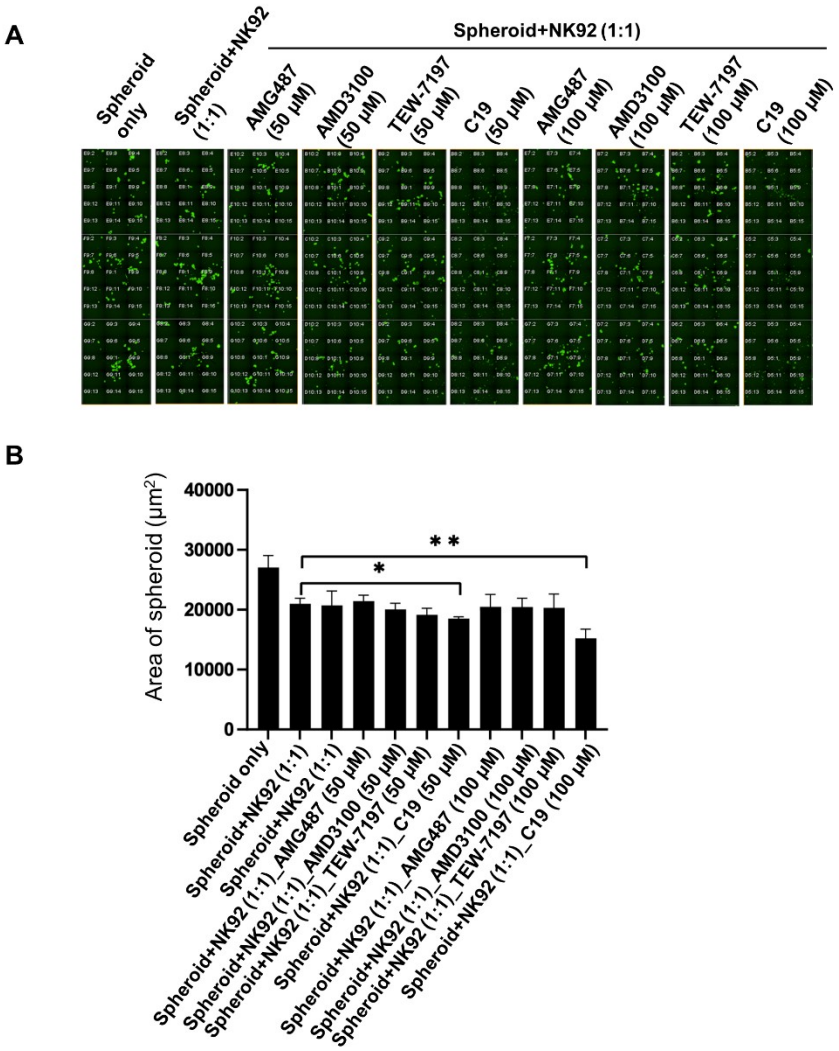

Figure S5. Imaging-based high-content screening of combinatorial drugs with NK-92 cells for effective cancer treatment. (A) Fluorescence images of GFP-overexpressing 110621 spheroids were exhibited under co-culture of NK-92 cells with various chemical drugs. (B) A quantitative graph showing the area of GFP spheroids. The *p* values were determined using a one-way ANOVA test followed by Tukey's multiple comparison test. **p* <0.05; ***p* <0.01.

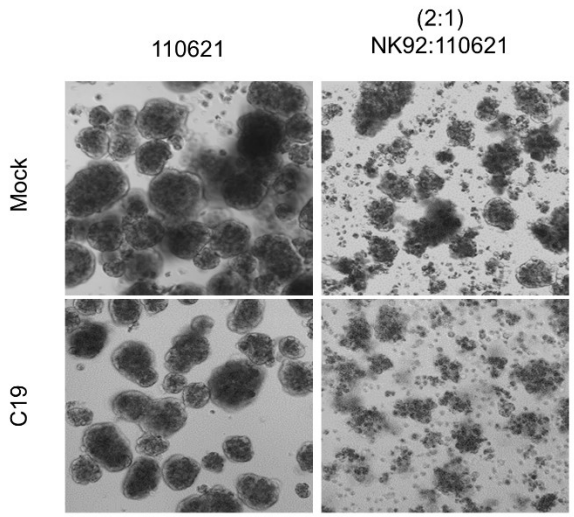

Figure S6. Co-treatment with C19 revealed significantly enhanced NK-mediated cytolysis Morphology observation of NK-92-mediated cancer killing under the treatment of C19.

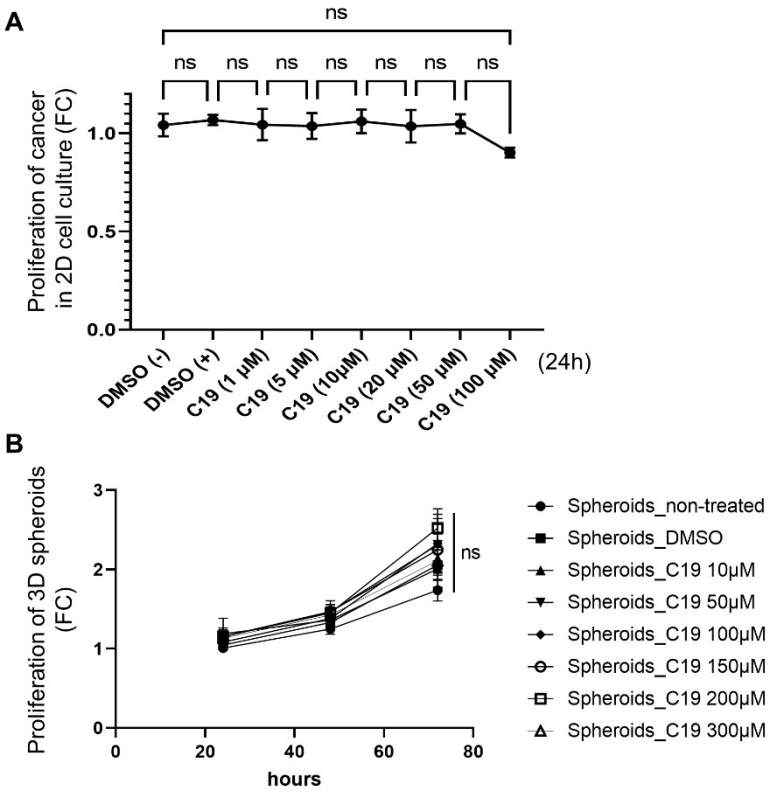

Figure S7. Proliferation comparison of 2D 110621 cancer cells and 3D 110621 spheroids in a C19 dose-dependent manner. The *p* values were determined using a one-way ANOVA test followed by Tukey's multiple comparison test. **p* <0.05; ***p* <0.01; ****p* <0.001.

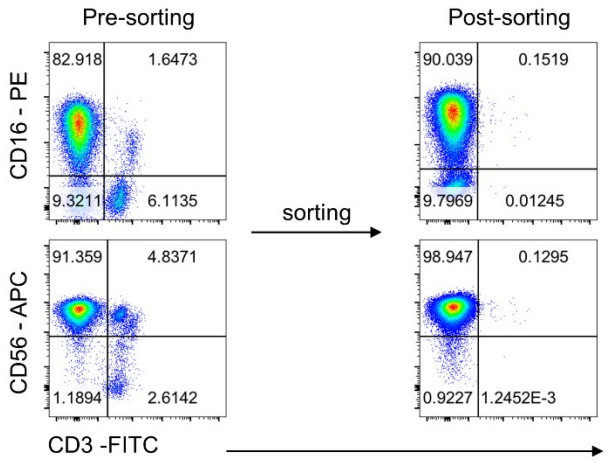

Figure S8. *In vitro* expansion and isolation of human PBNK cells. The PBMC cells were co-cultured with irradiated K562 feeder cells for 3 weeks and expanded PBNK cells were isolated for further experiments. The purity of PBNKs were analyzed by FACS analysis.

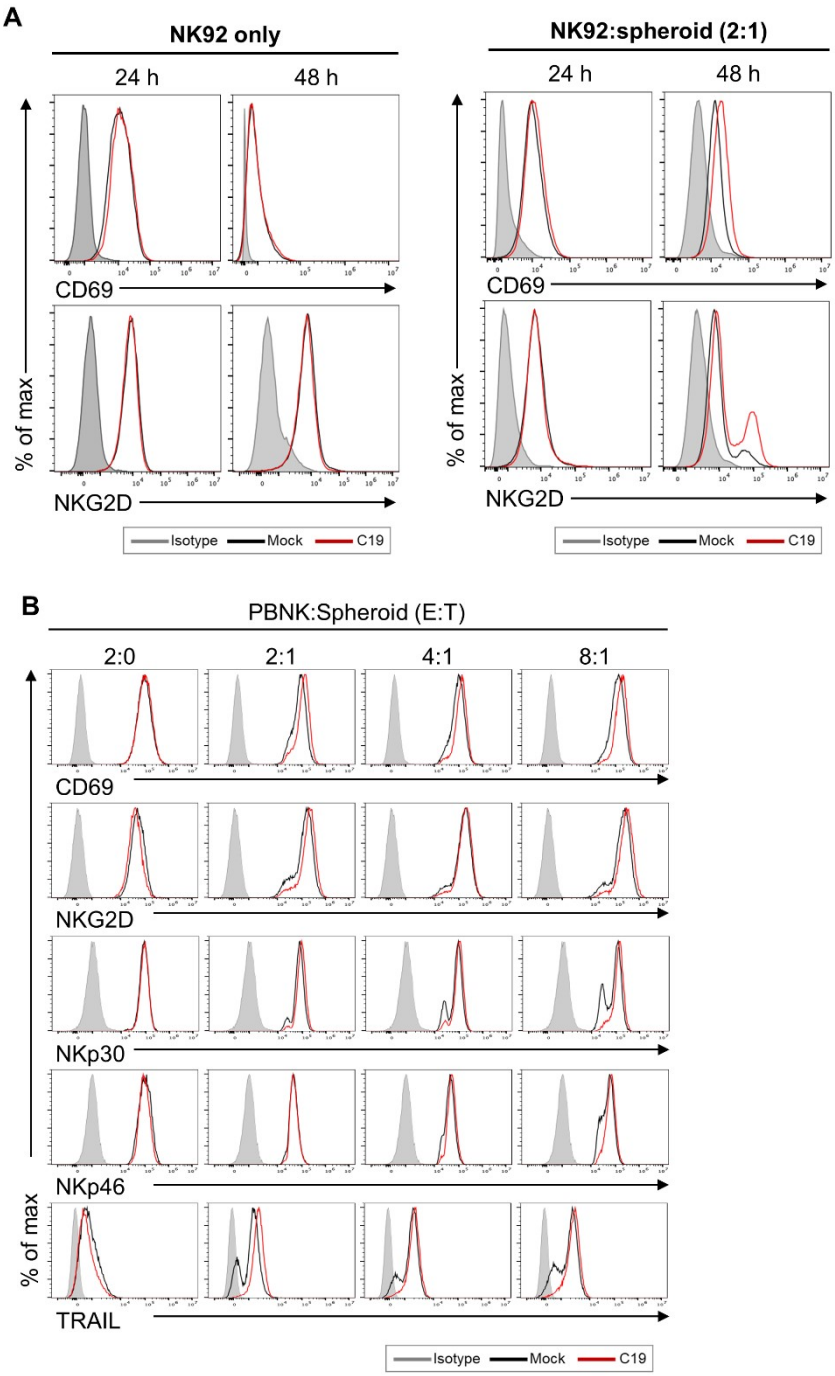

Figure S9. C19 induces activation of NK cells co-cultured with spheroid by flow cytometry. (A) Representative histograms show the levels of CD69 or NKG2D on only NK92 cells (left) and with spheroid (right) at a 2:1 effector:target ratio after 24 hours or 48 hours with C19. (B) Representative histograms show the level of PBNK cell activating markers.

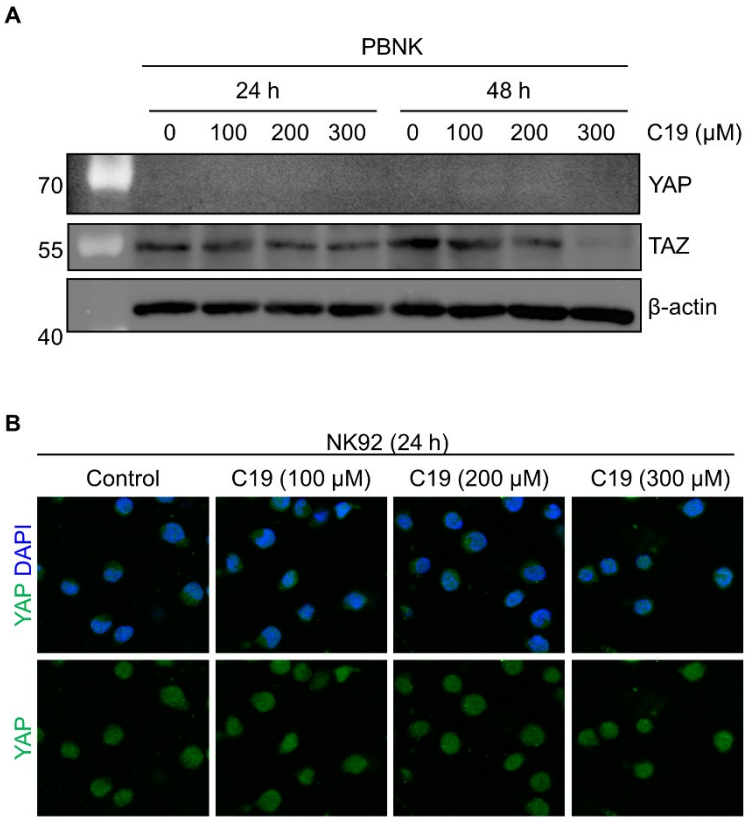

Figure S10. (A) Expression of YAP/TAZ in PBNK cells upon treatment with C19 in a dose-dependent manner. (B) Fluorescence images of YAP protein in NK92 cells were exhibited with treatment of various concentration of C19.

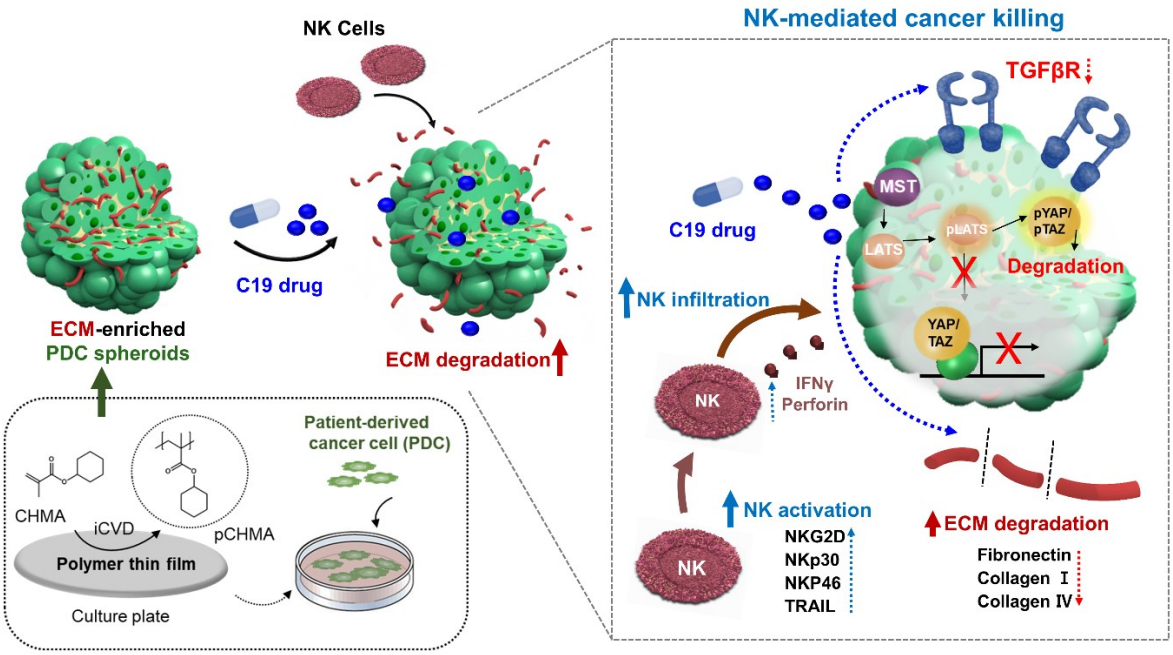

Figure S11. 3D multicellular tumor spheroids from pancreatic cancer patient-derived cancer cells (PDCs) generated on poly (cyclohexyl methacrylate) (pCHMA)-coated culture plate were co-cultured with NK-92 or primary NK (PBNK) cells in the presence of different chemical drugs at a 96-well plate format. Through our 3D co-culture system, we discovered a small drug, C19, for synergistic NK-mediated cytolysis against pancreatic cancer patient-derived cancer spheroids.

Table S1. The list of primers used for qRT-PCR analysis.

Primers	**Sequence (5`-3`)**
ALDHA1A1-F	CGCCAGACTTACCTGTCCTA
ALDHA1A1-R	GTCAACATCCTCCTTATCTCCT
CD133-F	ACCAGGTAAGAACCCGGATCAA
CD133-R	CAAGAATTCCGCCTCCTAGCACT
CD24-F	GCTCCTACCCACGCAGATTTAT
CD24-R	AGTTGGAAGTACTCTGGGAGGA
EPCAM-F	CAATGCCAGTGTACTTCAGTTGG
EPCAM-R	GCCATTCATTTCTGCCTTCATCA
TGFβ1-F	TTGTGCGGCAGTGGTTGA
TGFβ1-R	CCGTTGATGTCCACTTGCAG
TGFβ2-F	GGTGCTCTGTGGGTACCTTG
TGFβ2-R	AGGGTCTGTAGAAAGTGGGC
TGFβ3-F	ATCCTTCGGCCAGATGAGC
TGFβ3-R	CCACTCACGCACAGTGTCA
TGFβR1-F	GCCGTTTGTATGTGCACCC
TGFβR1-R	GCAATGGTCCTGATTGCAGC
TGFβR2-F	TGCCCCAGCTGTAATAGGAC
TGFβR2-R	TGGAAACTTGACTGCACCGT
TGFβR3-F	GGTTGGCCAGATGGTTATGA
TGFβR3-R	ATTTCAGGTCGGGTGAACAG
CXCR3-F	CAGGTGCCCTCTTCAACATCAA
CXCR3-R	TAGAGCTGGGTGGCATGAACTA
CXCR4-F	TCCATTCCTTTGCCTCTTTTGC
CXCR4-R	CAGGGTTCCTTCATGGAGTCAT
CXCR7-F	CACGTCTGCGTCCAACAATGA
CXCR7-R	AATGGAGAAGGGAACGGCAAAG
CXCL10-F	TGCCATTCTGATTTGCTGCCTTAT
CXCL10-R	TGCAGGTACAGCGTACAGTTCT
CXCL11-F	TGCTACAGTTGTTCAAGGCTTCC

CXCL11-R	AGGCTTTCTCAATATCTGCCACTTT
CXCL12-F	GCTTTCTCCAGGTACTCCTGAATC
CXCL12-R	CCAGGTACTCCTGAATCCACTTTAG